Available online at www.sciencedirect.com
ScienceDirect
High Energy Density Physics 3 (2007) 272–277
High Energy Density Physics
www.elsevier.com/locate/hedp

Correlation effects and their influence on line broadening in plasmas: Application to H_α

E. Stambulchik [a,*], D.V. Fisher [a], Y. Maron [a], H.R. Griem [b], S. Alexiou [c]

[a] Faculty of Physics, Weizmann Institute of Science, Rehovot 76100, Israel
[b] Institute for Plasma Research, University of Maryland, College Park, MD 20742, USA
[c] University of Crete, TETY, 71409 Heraklion, TK2208, Greece

Available online 7 February 2007

Abstract

In the last two decades, several computational approaches for the Stark broadening in plasmas have been developed, where the motion of both ions and electrons is simulated and their fields are approximated by using an effective Debye–Yukawa potential. This approximation, in general, should be questioned when the number of plasma particles in the Debye sphere is about unity or below. For testing the applicability of this approximation, molecular-dynamics simulations were performed, with all plasma particles interacting by the Coulomb potential, and the correlations in the motion of the particles were analyzed. It was found that even for a moderately coupled plasma ($N_e = 10^{18}$ cm^{-3}, $T = 1$ eV, where the number of electrons in the Debye sphere is ≈ 1.7), the collective effects play a significant role in the statistical and dynamical properties of the microfields. Nevertheless, the corrections to the H_α profile are rather small. We also show that accounting for transitions with $\Delta n \neq 0$ is crucial for proper determination of the shift, and to a lesser extent also of the width, of the spectral line.

Keywords: Stark effect; Correlation effects; Spectral line broadening

1. Introduction

Correlations between plasma particles have a significant effect on the Stark broadening of spectral lines in non-ideal plasmas. Corrections to the Holtsmark microfield distribution [1], which is valid in the ideal-plasma limit, have been employed since the studies of Mozer and Baranger [2] and Hooper [3]. A convenient parameter to characterize the deviation of a plasma from ideality is the coupling parameter Γ, defined for a single-species gas of charged particles with charge z_s and temperature T as

$$\Gamma_s = \frac{z_s^2 e^2}{r_s k_B T}, \tag{1}$$

where e is the electron charge, k_B is the Boltzmann constant, and the mean interparticle distance r_s is related to the particle density N_s by $r_s = (4\pi N_s/3)^{-1/3}$. This expression can be rewritten as

$$\Gamma_s = \frac{1}{3}\left(\frac{r_s}{\lambda_s}\right)^2, \tag{2}$$

where $\lambda_s = \sqrt{(k_B T/4\pi N_s e^2 z_s^2)}$ is the Debye length. In a weakly non-ideal plasma, the correction to the Coulomb field according to the Debye–Hückel theory [4] is well justified, yielding (in lieu of the Coulombic $F_C(r) = ez_s/r^2$)

$$F_D(r) = ez_s(1 + r/\lambda_s)\exp(-r/\lambda_s)/r^2. \tag{3}$$

A typical electric field $\overline{F}_D$ at $r = r_s$, for $r_s/\lambda_s \ll 1$, can be obtained by expanding Eq. (3):

$$\overline{F}_D \approx ez_s\left(1 - \frac{1}{2}(r_s/\lambda_s)^2\right)\Big/ r_s^2 = \left(1 - \frac{3}{2}\Gamma_s\right)\overline{F}_C. \tag{4}$$

The Debye screening will thus modify the linear Stark effect, i.e., $V = -z_s \vec{F}\vec{r}$ for a degenerate atomic system due

* Corresponding author.
E-mail address: evgeny.stambulchik@weizmann.ac.il (E. Stambulchik).

1574-1818/$ - see front matter © 2007 Elsevier B.V. All rights reserved.
doi:10.1016/j.hedp.2007.02.021

to the dipole interaction, resulting in a relative decrease by $|\Delta V/V| = (3/2)\Gamma_s$. Therefore, the corrections to the Stark line broadening due to the correlation effects are expected to be of the order of the coupling-parameter value. This simple analysis is readily generalized for one- or many-component plasmas, by introducing cross-coupling parameters. For example, it was found [5] that corrections to the widths of H- and He-like ion lines are of the order of the radiator-perturber cross-coupling $\Gamma_{r,\,p}$ (we note that the definition of Γ used in that reference differs from Eq. (1) by a factor of 3/2).

In addition to the modification of the quasistatic microfield distribution, the plasma correlations cause changes of the dynamic properties of the microfields, which also influence the line broadening. However, the Stark broadening usually depends rather weakly on a typical time scale of the perturbation (which results in a weak temperature dependence). This becomes especially apparent when overlapping collisions constitute a major part of the total perturbation as, e.g., takes place for high-n Balmer transitions [6].

The plasmas considered in Ref. [5] are weakly-coupled as a whole; it is only the coupling between the radiators, the high-Z ions that are assumed to be a minority component, and the rest of the plasma that is not negligible. This is typical for hot low-Z plasmas with traces of high-Z species, e.g., those used for the investigations of plasmas in heated-foam experiments [7]. A different situation occurs in low-temperature dense hydrogen plasmas, where the radiator–perturber interactions are negligible as the radiator is neutral, whereas the interactions between the perturbers and the corresponding correlation effects play an important role.

Let us assume the following plasma parameters: the electron density $N_e = 10^{18}$ cm^{-3}, and the electron and ion temperatures $T_e = T_i = 1$ eV. Then, the electron and ion plasma couplings are $\Gamma_e = \Gamma_i \approx 0.23$, and the number of particles in the Debye sphere is $N_D^{(e)} = N_D^{(i)} \approx 1.7$. Such values of the plasma coupling are approached in several measurements of H_α and H_β in warm dense plasmas [8–12]. For low-frequency components of the plasma microfields, which can be shielded efficiently by both electrons and protons, the corresponding values for the plasma as a whole (i.e., for the total density of the charged plasma particles $N_{tot} = 2N_e$) are $\Gamma_{tot} \approx 0.29$ and $N_D^{(tot)} \approx 1.2$. Therefore, corrections to the line widths and shifts of the order of 20–30% could be expected. However, for N_D approaching unity, the applicability of the Debye–Hückel theory becomes questionable.

2. Calculations

For the calculations a computer simulation method for the Stark broadening in plasmas [5] is employed, where two types of molecular-dynamics (MD) simulations are used to simulate the plasma microfields. In the first one, to be here referred to as the trivial MD (TMD) approach, the electron and proton perturbers move along straight line trajectories, and the field at the radiator is calculated as a sum of the Debye fields of all perturbers. The protons are assumed to be screened by both electrons and protons, so that their effective Debye length is $\lambda_e/\sqrt{2}$. In the second approach, full MD (FMD) simulations are performed, numerically solving a true N-body problem where all perturbers interact by Coulomb forces, and the field at the radiator is a sum of the Coulomb fields of all perturbers. The FMD simulations are described in detail in Refs. [13,14]. For the calculations presented here, the motion of 400 particles (200 electrons and 200 protons) was simulated in a cubic volume with mirror walls. The total time covered in the simulation was 2.6 ns, of which the first 0.1 ns was not used for the line shape calculations to allow for plasma thermalization. Monitoring the total energy of the simulated particles provided a check of the stability of the simulations. A minor, approximately linear in time, plasma heating was observed, resulting in a plasma temperature of $\approx$1.05 eV at the end of the simulation process which is due to the finite accuracy of the integration of the equations of motion.

In addition to the total field $\vec{F}_{tot}$ produced by all perturbers, the fields produced separately by ions ($\vec{F}_i$) and electrons ($\vec{F}_e$) were also recorded; clearly $\vec{F}_{tot} = \vec{F}_i + \vec{F}_e$. These field components were used for the correlation analysis presented. In both TMD and FMD simulations, the radiator is assumed to remain at the center of the simulation volume; the motion of the radiator is accounted for by assigning reduced masses to the perturbers. In solving the Schrödinger equation for the radiator, only the dipole terms in the perturbation Hamiltonian were retained. The inaccuracies associated with these assumptions are rather small for the plasma conditions assumed here, as will be discussed below.

Obviously the FMD approach is more computationally expensive, with the run time typically exceeding that of TMD by $O(N)$, where N is the number of particles in the simulation. Therefore, if the use of the TMD calculations can be justified, significantly faster Stark-broadening calculations become possible.

3. Results and discussion

3.1. Collective correlation effects

In Fig. 1 we present a comparison between the H_α line shapes calculated using the fields produced by the TMD and FMD simulations. Also given in the figure are line shapes calculated with the ion $\vec{F}_i$ and the electron $\vec{F}_e$ fields only. We note that in the case of the FMD simulation, these partial fields were obtained including in the simulation *both* ions and electrons, and accounting for interactions between them.

In the figure we observe that the FMD simulations yield larger broadening than the TMD in all cases, e.g., for electron broadening the FMD FWHM is larger than the TMD FWHM by $\approx$40%. However, the widths for the case when both electrons and ions are included differ by about $\sim$6%. The source of this apparent contradiction is a correlation between the motion, and, therefore, the fields, of electrons and ions. To investigate this in more detail we consider the static probability distribution functions of F_{tot}, F_i, and F_e in the TMD and FMD simulations, shown in Fig. 2. Here the probability distribution functions of the total fields are rather similar, however, the partial electron and ion fields in the FMD simulation are

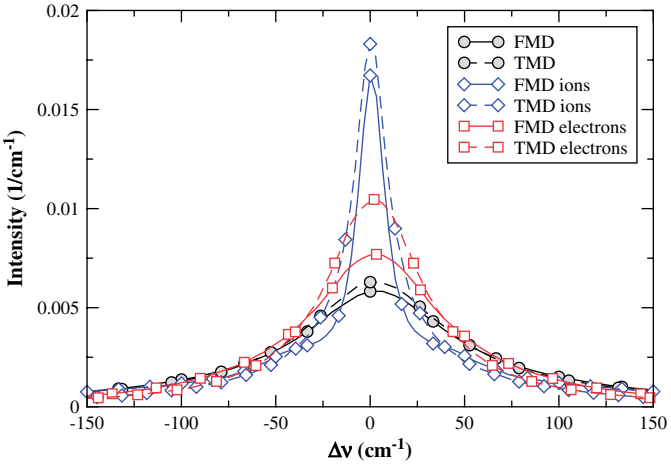

Fig. 1. Comparison of the FMD and TMD results. The contributions of ions and electrons are given separately. The line shapes are area-normalized. Here and in the other figures, $N_e = 10^{18}$ cm^{-3} and $T_e = T_i = 1$ eV are assumed.

weighted toward higher fields than in the TMD simulation. For example, while the FMD electron fields are weaker than in the ideal-plasma limit given by the Holtsmark function, they are nonetheless significantly stronger than the fields of the singly shielded Debye quasi-particles, e.g., the distribution of the TMD F_e. The difference between the FMD and TMD ion fields is even larger.

We note that the FMD ion and electron microfield distributions are identical. Indeed, since the fields are "measured" on a neutral radiator, the probability of a configuration of ions and electrons is equal to that of the same configuration with the ions and electrons exchanged, provided that the absolute values of the charges and the energy distributions of ions and electrons are the same, as is the case for the plasma considered here. Therefore, statistically, one may say that the electrons shield the ions exactly like the ions shield the electrons.

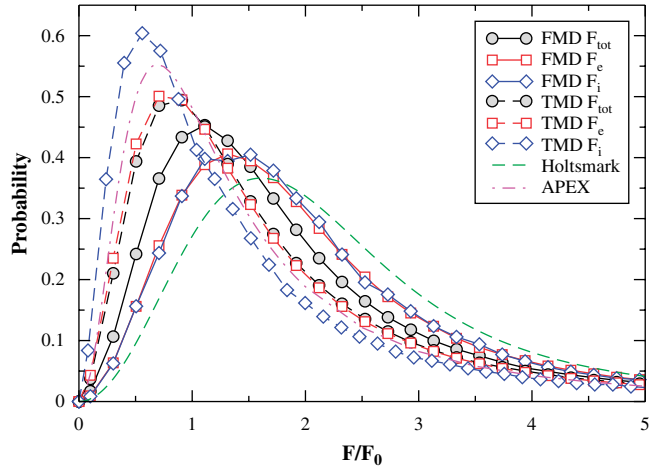

Fig. 2. Comparison of the FMD and TMD microfield distributions. The distributions of the total fields are scaled to the Holtsmark constant F_0 corresponding to the total density $N_{tot} = 2N_e$. The Holtsmark and the APEX-calculated ion microfield distribution functions are also given.

On the other hand, the ion and electron field dynamics are rather different, which can be illustrated using the field correlation functions

$$C_{ab}(\tau) = \int \mathrm{d}t\, \vec{\phi}_a(t) \cdot \vec{\phi}_b(t+\tau), \tag{5}$$

where

$$\vec{\phi}_a(t) = \frac{\vec{F}_a(t)}{F_a(t)}, \tag{6}$$

and the indices a and b represent either electrons (e) or ions (i). These auto- and cross-correlation functions are given in Fig. 3.

Both C_{ii} and C_{ee} show similar behavior: constant for short times and then dropping sharply. In fact, the typical "threshold" times $\tau_i \approx 300$ fs and $\tau_e \approx 7$ fs satisfy the expected relation $\tau_i/\tau_e = \sqrt{m_p/m_e}$. However, C_{ee} falls to a finite value (≈ 0.1); it approaches zero only at $t \approx \tau_i$. This is clearly due to electron–ion correlations indicated by $C_{ei}(\tau)$. Here, a significant *anti*-correlation between $\vec{F}_i$ and $\vec{F}_e$ is seen.[1]

A simple model can be used to explain these results. Let us assume that the electron field $\vec{F}_e$ acquires, due to the electron–ion correlations, a part of the ion component

$$\vec{F}_e = \vec{F}_{\bar{e}} + \alpha \vec{F}_i, \tag{7}$$

where $\vec{F}_{\bar{e}}$ and $\vec{F}_i$ are independent (i.e., $C_{\bar{e}i} = 0$). Then

$$C_{ee} = C_{\bar{e}\bar{e}} + \alpha^2 C_{ii}. \tag{8}$$

It is readily seen that for $\tau_e \ll \tau \ll \tau_i$

$$C_{ee}(\tau) \approx \alpha^2 C_{ii}(\tau), \tag{9}$$

and thus, for $\alpha^2 \ll 1$

$$\alpha \approx -\sqrt{C_{ee}(\tau)/C_{ee}(0)} \approx -0.3. \tag{10}$$

Therefore, $|\alpha|$ is of the order of Γ, as expected and is a result of Debye screening. Any motion of the relatively slow ions near the radiator is partially compensated by the electrons. As a result, a part of the slowly changing ion field gets "imprinted" on the electron field.

We point out that the approach to the Debye shielding used in the present TMD simulation (single shielding of the electron fields and double shielding of the ion fields) results, quite plausibly, in a slightly underestimated fields. Indeed, the ion microfield distribution calculated using the adjustable-parameter exponential approximation (APEX) method [15] corresponds to fields that are stronger than the doubly shielded TMD ion fields; yet the singly shielded approximation for ions would result in fields which are too strong (see Fig. 2). An approach similar to that of APEX can perhaps be devised

[1] The noise at very large values of τ is likely due to a poor statistic, since the larger τ the smaller is the number of the $\{F(t), F(t+\tau)\}$ pairs. In addition, artifacts due to the ions bouncing off the walls of the simulation volume are also possible.

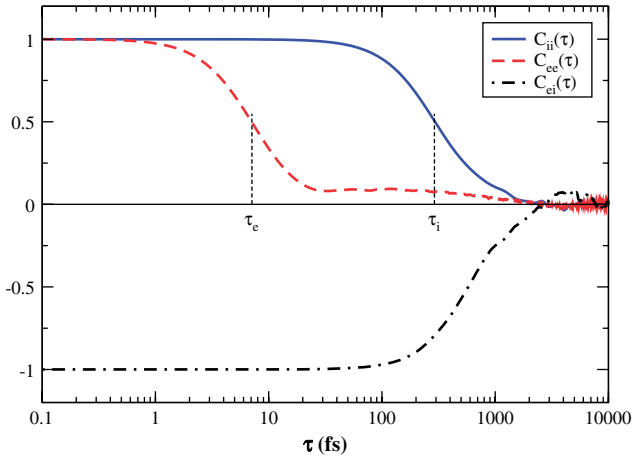

Fig. 3. Correlation between the FMD field components normalized such that $|C(0)| = 1$. Typical electron and ion correlation times τ_e and τ_i are indicated.

with respect to the effective Debye length as assigned to the TMD quasi-particles, which can result in an even better agreement between the TMD- and FMD-based Stark line shape calculations.

3.2. Three-body correlations

The plasma correlations are complex and essentially collective effects. Analyzing only a subset of these correlations without reference to the total context (in particular, neglecting the Debye screening effects) may, in general, be misleading. Nevertheless, attempts to refine Stark-broadening calculations by considering three-body correlations, namely the so-called "Acceleration of Electrons by Ion Field" (AEIF) phenomenon [16], have been made. Briefly, the argument is that a nearest-neighbor (NN) ion alters the trajectories and velocities of electrons passing near a radiator, and these changes are responsible for a reduction of the width and shift of spectral lines. This led to significant reductions in the case of H_α that were claimed even for values of the plasma coupling parameter that are lower than that considered here. First, and most straightforwardly, there are also effects which were neglected that are similar in magnitude, e.g., the altering of electron trajectories due to an NN electron. Second, it was shown [17–19] that the corrections are much smaller and, in fact, of the opposite sign. However, this issue remains unresolved [20,21].[2]

A true MD simulation, i.e., allowing *all* perturbers to move, cannot model the AEIF effect given the restrictive set of assumptions in Ref. [16], namely, a single static NN ion at a given distance $\vec{R}$ from the radiator. Instead, to resolve the issue we employ a variant of the TMD simulation run for electrons only in which a single ion is placed at a distance $\vec{R}$ from the origin (where the radiator resides), and the interactions between the NN ion and the electrons (but not between the electrons themselves) are allowed. The field at the radiator is a sum of the Debye fields of all the electrons and the NN ion field. Then, another simulation is performed, this time with the interaction between the electrons and the NN ion switched off (so that the only effect of the NN ion is its $\vec{F}_{\rm NN} = -(|e|\vec{R}/R^3)$ contribution to the total field). A set of such simulations was repeated for several values of R; the results of a pair of runs are given in Fig. 4. It is seen that the interactions between the NN ion and the electrons make the line broader, with the FWHM value increasing by almost 30%. Another feature seen in the figure is a tiny decrease of the static Stark splitting due to the electron–NN ion interactions. This is a result of the screening, similar to the Debye effect.

The FWHM values with and without AEIF as a function of the NN ion field are presented in Fig. 5. For weaker fields (of the order of the Holtsmark field F_0), corresponding to NN ion distances comparable to the inter-ion spacing, the corrections ($\sim$1%) are practically negligible. For stronger fields, the effect is more pronounced, however, the probability of such fields, decreasing as $\sim(F/F_0)^{-5/2}$, is very low. Therefore, the net effect after averaging over F is a minor *extra* broadening, and should be even weaker for smaller values of Γ. This confirms the previous analysis [17–19].

3.3. $\Delta n \neq 0$ corrections

It has been shown theoretically [22] and confirmed by numerical calculations [23] that in the case where energy levels are pure-degenerate, i.e., neglecting interactions between levels with different principal quantum numbers and neglecting the spin–orbit interactions, and assuming the dipole approximation and the independence of the density matrices of the radiator and the perturbers, the Stark shift is identically zero. In this work, we investigated the influence of the $\Delta n \neq 0$, called "quenching", interactions numerically. The FMD results are presented in Fig. 6, where the shift and FWHM values are also given. Here, the shifts were determined

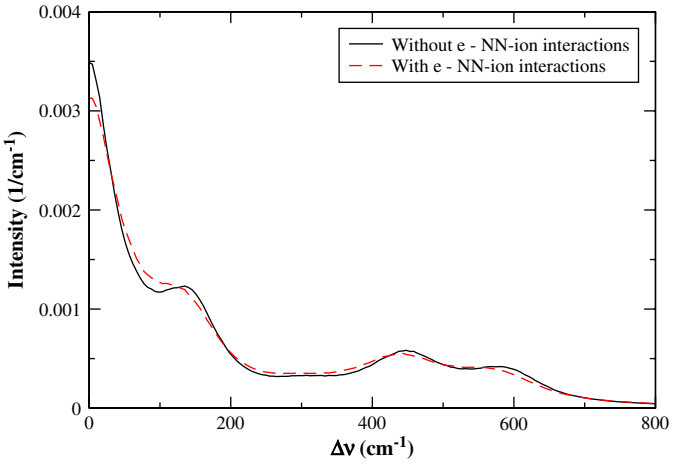

Fig. 4. Comparison of H_α line shapes obtained with the interactions between the electrons and the NN ion switched on and off. The NN ion (proton) is placed at $R = 2.5 \times 10^{-7}$ cm from the radiator.

[2] The "Conventional Theory" Stark widths in Figs. 1 and 2 of Ref. [21] are half widths at half maximum (HWHM), rather than FWHM, i.e., they should have been multiplied by a factor of two before comparison with the new results.

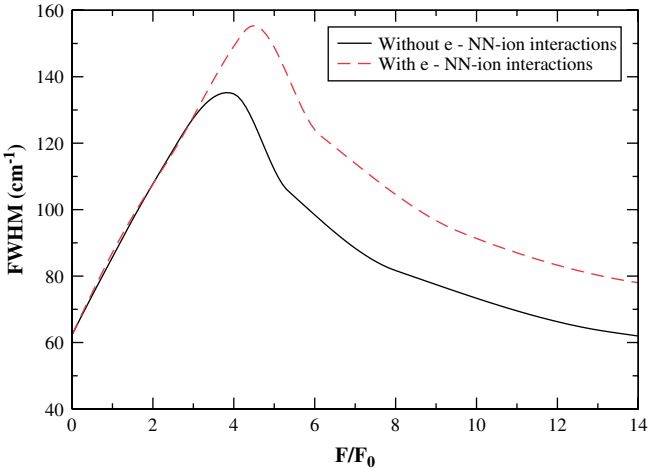

Fig. 5. The AEIF correction as a function of the NN ion field.

as the mean weighted detunings $\int \nu L(\nu)\mathrm{d}\nu$. When the quenching interactions are excluded, there is no shift of the line, thus confirming the previous findings. When the interactions between the initial and final levels of the transition are allowed, a small blue shift is observed, with a negligible change in the line width. The negligible influence on the line width of the interactions between the $n=2$ and $n=3$ levels is not surprising, given that the temperature of the perturbers is well below the energy separation between the levels. When the $n=4$ states are added to the Hamiltonian, the shift of the line changes its sign, and a noticeable ($\approx 8\%$) increase of the width is seen. A further addition of the $n=5$ states has a less pronounced effect. Since the complexity of the calculations growths dramatically with n, calculations with $n>5$ were not performed. However, assuming that the contribution of the high-n levels scales asymptotically as $\sim 1/n^3$, the effect of levels with $n>5$ would result in a minor increase of the absolute value of the line shift (about 10%) and in a practically negligible increase of the line width.

Therefore, while for the line shift the $\Delta n \neq 0$ corrections are crucial, the width of the H_α line is affected rather weakly even for the relatively high plasma density. Furthermore, except for the shift of the line as a whole, only a minor asymmetry in the line core is observed (see Fig. 7, where shifts at different relative to peak intensities are plotted). At the very far "blue" wing, $\Delta\nu > 10$ FWHM, where the line intensity falls below 1% of the peak value, the admixture of the "red" H_β wing breaks the line symmetry, as shown in Fig. 8. In the figure one also sees the effect of the quenching transitions on the H_β line shape, resulting mostly in slightly different peak amplitudes, as expected [24]. We note that stronger corrections to the H_β shape due to the quenching transitions even at significantly lower densities were previously reported [25]. However, we were unable to reproduce these results, and it is believed [26] that a computational problem in Ref. [25] could be responsible for the disagreement. We also note that, because no states with $n>5$ were included in the calculations, the H_γ line shape (also shown in Fig. 8), and especially its "blue" wing, may be inaccurate. In fact, for such a high density, the H_γ transition practically merges with the continuum because of the plasma continuum lowering.

3.4. Accuracy of the calculations

The total numerical errors of the line widths and shifts presented here are believed to be within 3% and 10%, respectively. The method used to evaluate the calculation accuracy is the same as in Ref. [6].

The use of a static radiator placed at a fixed point in the simulation volume introduces a certain inaccuracy, largely due to an underestimate of the ion dynamics effect. In trivial MD simulations one compensates for this by ascribing reduced masses to the perturbers. We performed the TMD calculations twice, assuming for the protons $\mu=1$ and then a reduced mass $\mu^*=0.5$. In the latter case, the H_α widths are larger by about 5%, with no noticeable change in the shifts. Since the correction is rather small and the TMD and FMD results are very close, we believe that corrections of the same order should be applied to the FMD widths to account for the motion of

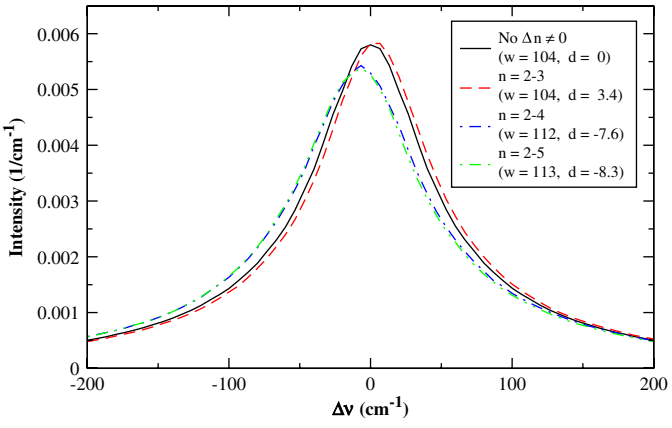

Fig. 6. Influence of the interactions between quantum states with different n on the H_α shape.

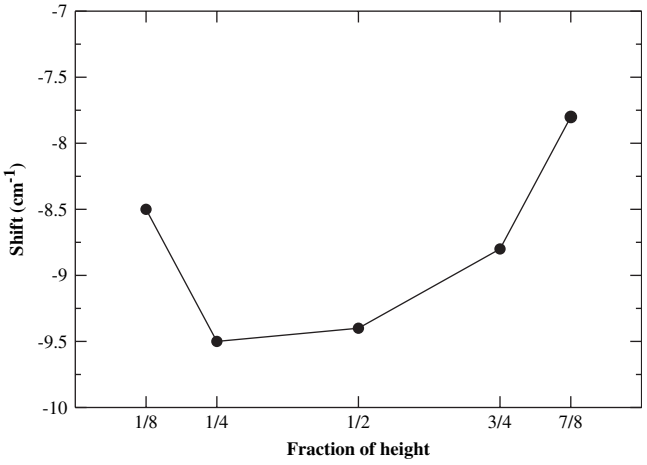

Fig. 7. H_α line shifts at different relative (to peak) intensities.

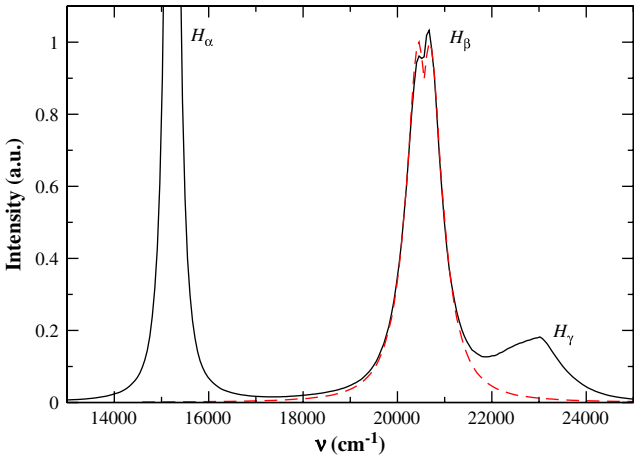

Fig. 8. The effect of quenching transitions between states with $2 \le n \le 5$ on the line shape of H_β. The H_β profile without the quenching transitions is shown by the dashed line.

the radiator. The widths given in the legend of Fig. 6 are corrected thusly.

The steady continuous plasma heating in the FMD plasma simulation, resulting from the finite accuracy of the N-body calculations, as mentioned in Section 2, is of less concern. This weak, $\approx 2.5\%$ on average, increase of the temperature during the process of the line shape calculations can be responsible for a line width inaccuracy of $\sim 1\%$.

Finally, we note that the higher-than-dipole multipole interactions and the influence of the radiator–perturber interactions on the distribution function of the perturbers [27] were neglected in the present calculations. For conditions considered here, the effect of these phenomena on the line width are rather minor. However, the respective corrections to the line shift [28,29] are more significant, amounting in total to about 15%. Note that these two contributions to the line shift act in the opposite directions, and thus partially cancel.

4. Conclusions

The influence of plasma correlation effects on the line shape of the H_α transition was analyzed. In the intermediate plasma coupling regime (the number of particles in the Debye sphere ≈ 1), using the trivial molecular dynamic calculations with non-interacting Debye–Yukawa quasi-particles produces rather accurate results. Accounting for the transitions with $\Delta n \neq 0$ is crucial for proper determination of the shift, and to a lesser extent of the width, of the spectral line.

Acknowledgements

We are thankful to R.W. Lee for valuable discussions and comments. This work was partly supported by the U.S.–Israel Binational Science Foundation, the Minerva Foundation (Germany), and the DOE University Excellence Center (USA).

References

[1] J. Holtsmark, Ann. Phys. (Leipzig) 58 (1919) 577.
[2] B. Mozer, M. Baranger, Phys. Rev. 118 (1960) 626.
[3] C.F. Hooper, Phys. Rev. 165 (1968) 215.
[4] P. Debye, E. Hückel, Z. Physik 24 (1923) 185.
[5] E. Stambulchik, Y. Maron, J. Quant. Spectrosc. Radiat. Transfer 99 (2006) 730–749.
[6] E. Stambulchik, S. Alexiou, H.R. Griem, P.C. Kepple, Phys. Rev. E 75 (2007) 016401.
[7] J. Bailey, G. Chandler, G. Rochau, Y. Maron, S. Slutz, G. Dunham, I. Golovkin, P. Lake, R. Lemke, J. Lucas, J. MacFarlane, T. Mehlhorn, T. Moore, D. Schroen, E. Stambulchik, K. Youngblood, High Energy Density Phys. 1 (2005) 21–30.
[8] Y. Vitel, J. Phys. B 20 (1987) 2327.
[9] S. Böddeker, S. Gunter, A. Könies, L. Hitzschke, H.-J. Kunze, Phys. Rev. E 47 (1993) 2785–2791.
[10] S. Büscher, T. Wrubel, S. Ferri, H.-J. Kunze, J. Phys. B 35 (2002) 2889–2897.
[11] S.A. Flih, E. Oks, Y. Vitel, J. Phys. B 36 (2003) 283.
[12] C.G. Parigger, D.H. Plemmons, E. Oks, Appl. Optics 42 (2003) 5992.
[13] D.V. Fisher, Y. Maron, Eur. Phys. J. D 14 (2001) 349.
[14] D.V. Fisher, J. Phys. B 36 (2003) 4107.
[15] C. Iglesias, J. Lebowitz, D. McGowan, Phys. Rev. A 28 (1983) 1667.
[16] E. Oks, J. Quant. Spectrosc. Radiat. Transfer 65 (2000) 405.
[17] H.R. Griem, J. Halenka, W. Olchawa, J. Phys. B 38 (2005) 975.
[18] H.R. Griem, J. Halenka, W. Olchawa, J. Phys. B 39 (2006) 1.
[19] S. Alexiou, H.R. Griem, J. Halenka, W. Olchawa, J. Quant. Spectrosc. Radiat. Transfer 99 (2006) 238.
[20] E. Oks, J. Quant. Spectrosc. Radiat. Transfer 99 (2006) 252.
[21] E. Oks, in: E. Oks, M.S. Pindzola (Eds.), AIP Conference Proceedings, Spectral Line Shapes, vol. 874, AIP, New York, 2006, pp. 19–34.
[22] S. Alexiou, J. Quant. Spectrosc. Radiat. Transfer 81 (2003) 13–17.
[23] J. Halenka, Phys. Rev. E 69 (2004) 028401.
[24] H.R. Griem, Z. Physik 137 (1954) 280.
[25] R.W. Lee, E. Oks, Phys. Rev. E 58 (1998) 2441–2445.
[26] R.W. Lee, private communication.
[27] D.B. Boercker, C.A. Iglesias, Phys. Rev. A 30 (1984) 2771.
[28] H.R. Griem, Phys. Rev. A 28 (1983) 1596.
[29] H.R. Griem, Phys. Rev. A 38 (1988) 2943.